

## Derivation of new SAC/FEMA performance evaluation solutions with second-order hazard approximation

Dimitrios Vamvatsikos<sup>1,\*</sup>

<sup>1</sup> *Faculty of Civil Engineering, Institute of Steel Structures, National Technical University of Athens, Greece.*

### SUMMARY

A novel set of SAC/FEMA-style closed-form expressions is presented to accurately assess structural safety under seismic action. Such solutions allow the practical evaluation of the risk integral convolving seismic hazard and structural response by employing a number of idealizations to achieve a simple analytical form. The most heavily criticized approximation of the SAC/FEMA formats is the first-order power-law fit of the hazard curve. It results to unacceptable errors whenever the curvature of the hazard function becomes significant. Adopting a second-order fit, instead, allows capturing the hazard curvature at the cost of necessitating new analytic forms. The new set of equations is a complete replacement of the original, enabling (a) accurate estimation of the mean annual frequency of limit-state exceedance and (b) safety checking for specified performance objectives in a code-compatible format. More importantly, the flexibility of higher-order fitting guarantees a wider-range validity of the local hazard approximation. Thus, it enables the inversion of the formulas for practically estimating the allowable demand or the required capacity to fulfill any design objective. Copyright © 2012 John Wiley & Sons, Ltd.

Received . . .

**KEY WORDS:** seismic performance evaluation; SAC/FEMA; uncertainty; demand; capacity; probabilistic methods

### 1. INTRODUCTION

The Northridge 1994 earthquake shed light on the inferior performance of welded steel moment-resisting connections and became the catalyst for commissioning the SAC/FEMA project. This highly-influential project culminated in the FEMA-350/351 guidelines [1, 2] that became a milestone in earthquake engineering by popularizing the concept of evaluating the seismic performance of structures within a probabilistic framework. This is the legacy of Cornell *et al.* [3] who devised a ground-breaking closed-form solution for estimating the mean annual frequency (MAF) of limit-state exceedance and a simple safety checking inequality similar to the familiar Load and Resistance Factor Design (LRFD) format [4].

The SAC/FEMA MAF format offers a simple expression to convolve the seismic hazard with the structural response and estimate the mean annual rate (or the mean return period) of exceeding any limit-state that can be defined on the structural response. The effect of aleatory variability (caused by natural randomness) is directly included, while epistemic uncertainty (due to incomplete knowledge) can be treated with a user-selected level of confidence. Thanks to the simplicity of this formulation, it has found widespread recognition as a basis for performance evaluation of structures,

---

<sup>†</sup>E-mail: divamva@mail.ntua.gr

Contract/grant sponsor: EU Research Executive Agency; contract/grant number: PCIG09-GA-2011-293855

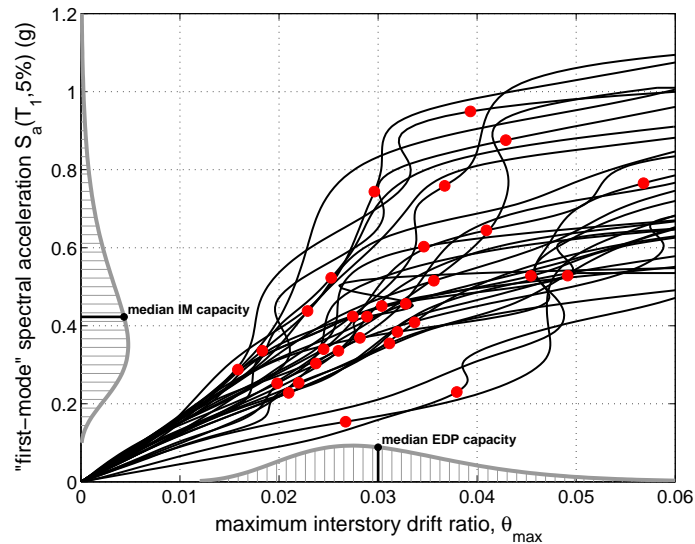


Figure 1. IDA curves and limit-state capacity points for a 9-story steel moment-resisting frame [8]. The lognormal distributions of the EDP and IM values of capacity are shown along the axes.

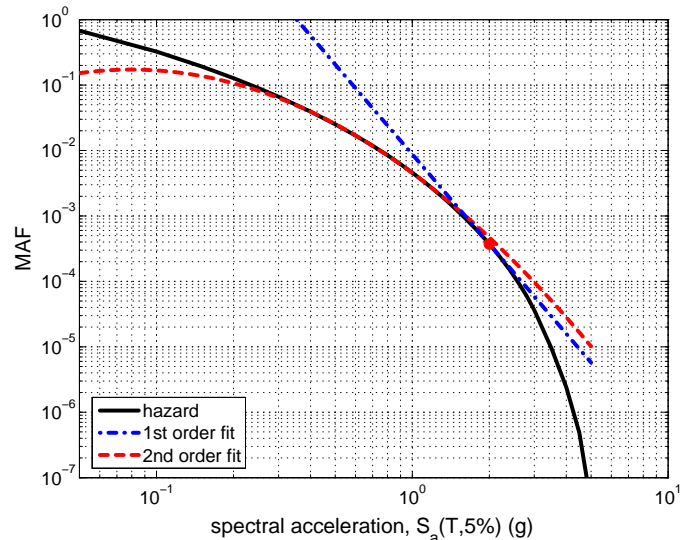


Figure 2.  $S_a$  hazard curve for  $T = 0.7$ s at Van Nuys CA and its first- and second-order fits via Equations (7) and (9) in the vicinity of  $S_a = 2$ g. The first-order equation has been fitted tangentially, while the second-order fit has been weighted with emphasis in the low MAF region [9].

both for assessment (e.g., Fajfar and Dolsek [5]) and design (Franchin and Pinto [6]). In principle, it can also be thought to have become the core of the Pacific Earthquake Engineering Research (PEER) Center probabilistic framework through the Cornell-Krawinkler framing equation [7].

The Demand-Capacity Factor Design (DCFD) format was introduced to allow the efficient verification of limit-state safety. While safety checking can also be achieved by comparing the limit-state MAF against a maximum allowable value, e.g., the typical 1/475yrs for Life-Safety, this requires comprehensive data on the distribution of structural response given intensity. Formally, one needs to estimate, at least in the region of interest, the distribution of the pertinent engineering demand parameter (EDP, e.g., the maximum interstory drift  $\theta_{\max}$ ) versus the seismic intensity, (IM, e.g., the 5%-damped first-mode spectral acceleration  $S_a(T_1, 5\%)$ ). Such detailed information may appear in the form of incremental dynamic analysis (IDA [10]) curves and corresponding limit-state

“capacity points” that represent the IM and EDP values to signal violation for each ground motion record (and model realization), as shown in Figure 1. The DCFD inequality is a simpler alternative, as it can be evaluated with a limited knowledge of the structural response and significantly reduced computational effort. By resembling the typical safety-checking LRFD inequality, it is a viable candidate for inclusion in seismic guidelines.

Despite the advantages of the SAC/FEMA analytic expressions, well-founded criticism has been expressed for their lack of accuracy, mainly by Aslani and Miranda [11] and Bradley and Dhakal [12]. The main issue raised is the adequacy of the approximations used in deriving the closed-form expressions. The most significant errors seem to stem from the power-law fitting of the seismic hazard curve. This is an approximation that quickly loses its accuracy whenever the seismic hazard function displays large curvatures, as shown in Figure 2, invariably introducing massive errors. In the following, we aim to rectify this by incorporating the effect of curvature in the SAC/FEMA formulation. A higher-fidelity second-order power-law hazard fit will thus be employed and new analytical expressions will be derived to offer unrestricted predictive ability regardless of the shape of the hazard function.

## 2. PROBABILISTIC BASIS

Let  $H(s)$  be the hazard function representing the MAF of exceeding a certain IM value equal to  $s$ . At any given value  $s$ , the rate of IM exceedance in its neighborhood  $[s, s + ds]$  is approximately constant:  $-dH(s)$ , the minus sign needed due to the monotonically decreasing hazard. This rate defines a “local” Poisson process of seismic events that exceed the designated level of IM. Another Poisson process can be derived for limit-state (LS) exceedance by filtering the process of seismic events (e.g., [13, 14]) by the probability of LS exceedance for a given  $s$ . Its “local” rate  $d\lambda_{LS}$  becomes

$$d\lambda_{LS}(s) = -P(C < D | s)dH(s), \quad (1)$$

where  $C$  is the capacity associated with the limit-state and  $D$  the corresponding demand generated by seismic loads. The conditional probability  $P(C < D | s)$  of limit-state exceedance, often termed the *fragility* or *vulnerability* function, can be calculated in two equivalent ways:

$$P(C < D | s) = P(s_c < s) = F(s_c | s), \quad (2)$$

or

$$P(C < D | s) = P(\theta_c < \theta | s). \quad (3)$$

In other words, a structure violates LS (a) if the IM of the earthquake is above its (random) IM-capacity  $s_c$  in Equation (2) or, equivalently, (b) if the (random) EDP demand  $\theta$  (at a given  $s$ ) exceeds the (random) EDP-capacity  $\theta_c$  in Equation (3).  $F(\cdot)$  represents the cumulative distribution function (CDF) of its argument. To understand the above formulations it is useful to visualize the cloud of capacity points associated with LS in the EDP-IM plane, each  $i$ -th point placed at its own  $(\theta_c^i, s_c^i)$  coordinates. For readers familiar with IDA [10] these can be represented by one point per IDA curve (ground motion record) that signifies the level above which the limit-state is violated, both in EDP and in IM terms (Figure 1). Equation (2) is straightforward to understand, as the level of IM, or  $s$ , is given and  $s_c$  is a random variable. Thus  $P(s_c < s)$  is simply the CDF of the IM-capacity evaluated at  $s$ , easily estimated from the cloud of capacity points in the EDP-IM plane. For example, we can just make the popular assumption of lognormality and estimate as distribution parameters the mean logarithm and standard deviation of the logarithms of the IM-ordinates of the capacity points. On the other hand, Equation (3) is more difficult to apply, as both  $\theta$  given  $s$  and  $\theta_c$  (independent of  $s$ ) are random variables.

With that in mind, let us now discuss the estimation of  $\lambda_{LS}$ . For both formulations, this can be done via a simple integration of  $d\lambda_{LS}(s)$  from Equation (1) over all values of  $s$ :

$$\begin{aligned}\lambda_{LS} &= \int_0^{+\infty} d\lambda_{LS}(s) = - \int_0^{+\infty} P(C < D | s) dH(s) \\ &= - \int_0^{+\infty} P(C < D | s) \frac{dH(s)}{ds} ds.\end{aligned}\quad (4)$$

If we attempt integration by parts (Jalayer [15]) we get

$$\begin{aligned}\lambda_{LS} &= - [P(C < D | s)H(s)]_0^{+\infty} + \int_0^{+\infty} \frac{dP(C < D | s)}{ds} H(s) ds \\ &= \int_0^{+\infty} \frac{dP(C < D | s)}{ds} H(s) ds.\end{aligned}\quad (5)$$

The constant first term above was removed as it becomes zero at both limits of 0 and  $+\infty$ : In the first case the probability of demand exceeding capacity is null for zero intensity. In the latter case, the hazard  $H(s)$  zeroes out for infinite intensities. In the following pages, we will deal exclusively with analytically solving Equation (5) both with an IM and an EDP basis for defining demand and capacity, essentially choosing between the alternative representations of Equations (2) and (3).

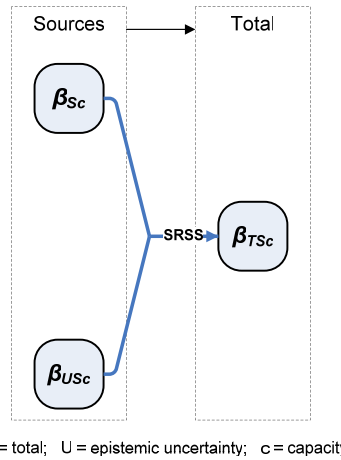


Figure 3. The breakdown of IM-basis dispersions and combination via SRSS (square-root sum of squares).

### 3. MEAN ANNUAL FREQUENCY FORMAT

#### 3.1. IM-basis

Let us assume that the IM-capacity  $s_c$  is lognormally distributed with median  $\hat{s}_c$  and dispersion (standard deviation of the log-data)  $\beta_{Sc}$ . Then,  $P(C < D | s)$  simply becomes the CDF of the limit-state IM-capacity. If  $\Phi(\cdot)$  represents the CDF of the standard normal distribution and given that the derivative of the CDF is the PDF (probability density function), Equation (5) becomes:

$$\begin{aligned}\lambda_{LS} &= \int_0^{+\infty} \frac{d}{ds} \left[ \Phi \left( \frac{\ln s - \ln \hat{s}_c}{\beta_{Sc}} \right) \right] H(s) ds \\ &= \int_0^{+\infty} \frac{1}{\sqrt{2\pi s} \beta_{Sc}} \exp \left[ -\frac{1}{2} \left( \frac{\ln s - \ln \hat{s}_c}{\beta_{Sc}} \right)^2 \right] H(s) ds.\end{aligned}\quad (6)$$

In the above we have also made use of the fact that for a lognormal variable, the mean of its logarithm is equal to the logarithm of the median [13]. A closed form solution to Equation (6) has been derived by Cornell *et al.* [3] by making a number of further idealizations.

First, the first-order assumption has been adopted, meaning that the epistemic uncertainty does not influence the median of the capacity,  $\hat{s}_c$ , only its dispersion. Thus, the latter can be attributed to aleatory randomness, i.e., record-to-record variability  $\beta_{Sc}$ , or to both aleatory and epistemic sources combined as  $\beta_{TSc}^2 = \beta_{USc}^2 + \beta_{Sc}^2$  (see Figure 3). This assumption may not be entirely accurate, as shown e.g., by Liel *et al.* [16] and Vamvatsikos and Fragiadakis [8], but it remains reasonable.

Furthermore, the hazard curve is locally approximated around the median capacity  $\hat{s}_c$ , by a power-law, or, equivalently, a straight line in log-log coordinates (see also Kennedy and Short [17]):

$$H(s) = k_0(s)^{-k_1} = k_0 \exp(-k_1 \ln s), \quad (7)$$

where  $k_0, k_1$  are positive real numbers, representing the intercept and the slope of the fitted line. Then, as shown by Jalayer [15], the MAF of exceeding a limit-state LS can be approximated as

$$\lambda_{LS} = H(\hat{s}_c) \exp\left(\frac{1}{2} k_1^2 \beta_{Sc}^2\right). \quad (8)$$

The proposed innovation relative to the above solution is to fit the hazard curve using a higher-fidelity second-order polynomial, rather than a linear function, in log-space (Figure 2):

$$H(s) = k_0 \exp(-k_2 \ln^2 s - k_1 \ln s), \quad (9)$$

with  $k_1, k_2 > 0$  and  $k_2 \geq 0$ , the latter indicating the (local) hazard curvature. To derive the new closed form expression, the exact same steps will be followed, as described in detail by Jalayer [15]: We will introduce the new hazard approximation of Equation (9) in Equation (6) and then attempt to form a complete square term in the exponential function, involving the integrand variable  $\ln x$ :

$$\begin{aligned} \lambda_{LS} &= \int_0^{+\infty} \frac{k_0}{\sqrt{2\pi s} \beta_{Sc}} \exp\left[-\frac{1}{2} \left(\frac{\ln s - \ln \hat{s}_c}{\beta_{Sc}}\right)^2 - (k_2 \ln^2 s + k_1 \ln s)\right] ds \\ &= \int_0^{+\infty} \frac{1}{\sqrt{2\pi s} \beta_{Sc}} \exp\left[-\frac{1}{2} \left(\frac{\ln s - \frac{\ln \hat{s}_c - k_1 \beta_{Sc}^2}{1 + 2k_2 \beta_{Sc}^2}}{\frac{\beta_{Sc}}{\sqrt{1 + 2k_2 \beta_{Sc}^2}}}\right)^2\right] ds \\ &\quad \cdot k_0 \exp\left\{-\frac{1}{2\beta_{Sc}^2} \left[\ln^2 \hat{s}_c - \frac{(\ln \hat{s}_c - k_1 \beta_{Sc}^2)^2}{1 + 2k_2 \beta_{Sc}^2}\right]\right\} \end{aligned} \quad (10)$$

If the integrand is multiplied by the square-root appearing in the denominator of the completed square, it will become the PDF of a lognormal distribution. Thus, its integral within  $[0, +\infty)$  is unity by definition. The above equation is then reduced to:

$$\begin{aligned} \lambda_{LS} &= \frac{k_0}{\sqrt{1 + 2k_2 \beta_{Sc}^2}} \exp\left\{-\frac{1}{2\beta_{Sc}^2} \left[\ln^2 \hat{s}_c - \frac{(\ln \hat{s}_c - k_1 \beta_{Sc}^2)^2}{1 + 2k_2 \beta_{Sc}^2}\right]\right\} \\ &= \frac{k_0}{\sqrt{1 + 2k_2 \beta_{Sc}^2}} \exp\left(\frac{-k_2 \ln^2 \hat{s}_c - k_1 \ln \hat{s}_c}{1 + 2k_2 \beta_{Sc}^2}\right) \exp\left(\frac{1}{2} \cdot \frac{k_1^2 \beta_{Sc}^2}{1 + 2k_2 \beta_{Sc}^2}\right) \end{aligned} \quad (11)$$

If we set

$$p = \frac{1}{1 + 2k_2 \beta_{Sc}^2}, \quad (12)$$

then, we can multiply and divide by  $k_0^p$  to transform the first exponential term into the hazard function value  $H(\hat{s}_c)$  corresponding to the median capacity. Equation (11) finally becomes:

$$\begin{aligned}\lambda_{LS} &= \sqrt{p} k_0^{1-p} [H(\hat{s}_c)]^p \exp\left(\frac{1}{2} p k_1^2 \beta_{Sc}^2\right) \\ &= \sqrt{p} k_0^{1-p} [H(\hat{s}_c)]^p \exp\left[\frac{k_1^2}{4k_2}(1-p)\right].\end{aligned}\quad (13)$$

The above expression contains all the fundamental elements that contribute to risk: The hazard value at the median capacity,  $H(\hat{s}_c)$ , multiplied by a larger-than-unity exponential factor to incorporate the effect of IM-capacity dispersion  $\beta_{Sc}$ . If there was no such variability, then the MAF of exceeding the limit-state would be equal to the MAF provided by the hazard at the (deterministic) IM-capacity. The difference of Equation (13) from the SAC/FEMA original is the introduction of  $p$ . Given the concave hazard shape,  $k_2 \geq 0$  and  $p \in (0, 1]$ , with values of  $p$  closer to one (rather than zero) being the norm in practice. If  $k_2$  is set to zero, then  $p = 1$  and our solution simplifies to the first-order format of Equation (8). In other words,  $p$  encapsulates the contribution of the hazard curvature, acting as a correction factor to reduce the effect of  $H(\hat{s}_c)$  and the exponential dispersion term. Essentially, it is a measure of the difference of the areas enclosed underneath the first- and second-order fits, shown in Figure 2. As the curvature, represented by  $k_2$ , and the capacity dispersion  $\beta_{Sc}$  increase, this discrepancy becomes more significant and  $p$  is accordingly lowered below 1.0. To account for this, Equation (13) is more complex than its predecessor, but, as we are going to discuss in the final section, this is more than made up for by its accuracy.

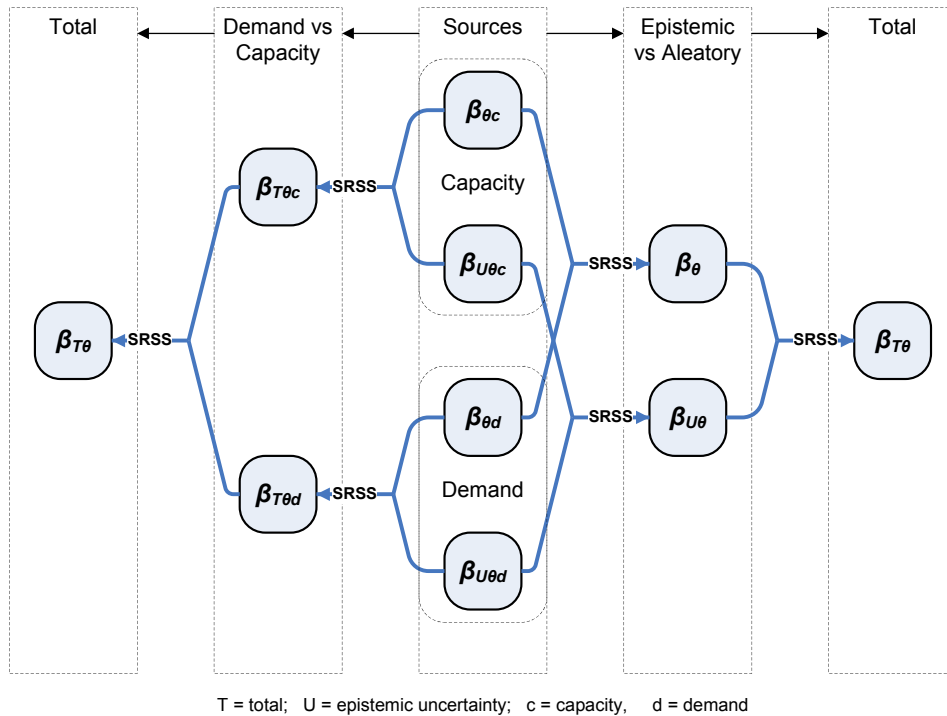


Figure 4. The breakdown of EDP-basis dispersions and their combinations via SRSS.

### 3.2. EDP basis

Following again in the footsteps of Jalayer [15], we are going to derive the EDP-based MAF format using the improved second-order polynomial approximation of Equation (9) for the hazard curve. To proceed, the EDP-capacity  $\theta_c$  is assumed lognormal with median  $\hat{\theta}_c$  and dispersions  $\beta_{\theta_c}$ ,  $\beta_{U\theta_c}$

due to aleatory and epistemic sources, respectively (Figure 4). Additionally, the EDP-demand given the IM is also taken as lognormal with dispersions of  $\beta_{\theta_d}$ ,  $\beta_{U\theta_d}$  independent of the level of IM and a conditional median  $\hat{\theta}(s)$  that depends on intensity via a power-law relationship. This is typically obtained by a linear regression in log-log coordinates and, in the framework of IDA it can be thought of being an approximation of the median IDA curve (see also Figure 8 later):

$$\hat{\theta}(s) \approx as^b. \quad (14)$$

Assuming we are not fitting close to the global-instability region (where the IDA curves become flat in Figure 1), collapse will not become an issue and the above equation can be used accurately enough. Then, Cornell *et al.* [3], show that Equation (5) becomes:

$$\lambda_{LS} = H \left[ \left( \frac{\hat{\theta}_c}{a} \right)^{\frac{1}{b}} \right] \exp \left[ \frac{k_1^2}{2b^2} (\beta_{\theta_d}^2 + \beta_{\theta_c}^2) \right]. \quad (15)$$

Same as before, the dispersions  $\beta_{\theta_c}$ ,  $\beta_{\theta_d}$  may be only aleatory or they can be replaced by their combined aleatory and epistemic counterparts  $\beta_{T\theta_c}$  and  $\beta_{T\theta_d}$ ; see Figure 4.

To derive an improved closed-form solution including the second-order approximation of Equation (9), we shall follow a two-step process [15]. First, we will assume that  $\theta_c$  is deterministic, i.e.,  $\beta_{\theta_c} = \beta_{U\theta_c} = 0$ . Then, the missing dispersion in capacity will be added.

**3.2.1. Deterministic EDP capacity** Starting from Equation (3), capacity now is  $C = \theta_c$  (assumed constant) compared versus the demand  $D = \theta$ . Noting that the logarithm is a monotonically increasing function and thus does not influence the inequality, we have

$$\begin{aligned} P(C < D | s) &= P(\ln \theta_c < \ln \theta | s) \\ &= 1 - \Phi \left( \frac{\ln \theta_c - \ln \hat{\theta}(s)}{\beta_{\theta_d}} \right) \end{aligned} \quad (16)$$

since  $\theta$  is assumed to follow a lognormal distribution defined by median  $\hat{\theta}(s)$  and dispersion  $\beta_{\theta_d}$  as discussed earlier. Then, following the same steps as before, we introduce Equation (16) into the integral of Equation (5):

$$\begin{aligned} \lambda_{LS} &= \int_0^{+\infty} \frac{d}{ds} \left[ 1 - \Phi \left( \frac{\ln \theta_c - \ln \hat{\theta}(s)}{\beta_{\theta_d}} \right) \right] H(s) ds \\ &= \int_0^{+\infty} \left\{ -\frac{d}{ds} \left[ \Phi \left( \frac{\ln \theta_c - \ln(as^b)}{\beta_{\theta_d}} \right) \right] \right\} H(s) ds \\ &= \int_0^{+\infty} \left\{ -\frac{d}{ds} \left[ \Phi \left( \frac{(\ln \theta_c - \ln a) - b \ln s}{\beta_{\theta_d}} \right) \right] \right\} H(s) ds \\ &= \int_0^{+\infty} \frac{1}{\sqrt{2\pi s}(\beta_{\theta_d}/b)} \exp \left[ -\frac{1}{2} \left( \frac{\ln s - (\ln \theta_c - \ln a)/b}{\beta_{\theta_d}/b} \right)^2 \right] H(s) ds. \end{aligned} \quad (17)$$

A chain rule was employed in the last step to differentiate  $\Phi(\cdot)$ , canceling the integrand's negative sign in the process and coming up with the PDF of a lognormal distribution.

Comparing to Equation (6), it becomes obvious that we only need to replace  $\beta_{S_c}$  with  $\beta_{\theta_d}/b$  and  $\ln \hat{s}_c$  with  $(\ln \theta_c - \ln a)/b$  to reach the obvious solution:

$$\begin{aligned} \lambda_{LS}(\theta_c) &= \sqrt{q} k_0^{1-q} [H(s_{\theta_c})]^q \exp \left( \frac{1}{2b^2} q k_1^2 \beta_{\theta_d}^2 \right) \\ &= \sqrt{q} k_0^{1-q} [H(s_{\theta_c})]^q \exp \left[ \frac{k_1^2}{4k_2} (1-q) \right], \end{aligned} \quad (18)$$



where

$$q = \frac{1}{1 + 2k_2\beta_{\theta_d}^2/b^2}, \quad s_{\theta_c} = \left(\frac{\theta_c}{a}\right)^{1/b}. \quad (19)$$

$s_{\theta_c}$  is the IM value corresponding to the deterministic capacity  $\theta_c$  according to the power-law approximation of Equation (14).

**3.2.2. Probabilistic EDP capacity** If  $\theta_c$  is a random variable, to find the MAF we need to integrate  $\lambda_{LS}(\theta_c)$  derived in Equation (18) for a given EDP capacity over all possible values of  $\theta_c$  times their probability of occurrence. For  $f(\cdot)$  symbolizing the PDF of its argument:

$$\begin{aligned} \lambda_{LS} &= \int_0^{+\infty} \lambda_{LS}(\theta_c) f(\theta_c) d\theta_c \\ &= \int_0^{+\infty} \sqrt{q} k_0^{1-q} [H(s_{\theta_c})]^q \exp\left(\frac{1}{2b^2} q k_1^2 \beta_{\theta_d}^2\right) f(\theta_c) d\theta_c \\ &= k_0 \sqrt{q} \exp\left(\frac{1}{2b^2} q k_1^2 \beta_{\theta_d}^2\right) \\ &\quad \cdot \int_0^{+\infty} \exp\left[-k_2 q \left(\frac{\ln \theta_c - \ln a}{b}\right)^2 - k_1 q \left(\frac{\ln \theta_c - \ln a}{b}\right)\right] f(\theta_c) d\theta_c. \end{aligned} \quad (20)$$

Assuming that  $\theta_c$  is lognormally distributed with median  $\hat{\theta}_c$  and dispersion  $\beta_{\theta_c}$ , we can simply follow the exact steps that we used previously for the IM case to arrive at the following solution:

$$\begin{aligned} \lambda_{LS} &= \sqrt{\phi} k_0^{1-\phi} [H(s_{\hat{\theta}_c})]^\phi \exp\left[\frac{1}{2b^2} q k_1^2 (\beta_{\theta_d}^2 + \phi \beta_{\theta_c}^2)\right] \\ &= \sqrt{\phi} k_0^{1-\phi} [H(s_{\hat{\theta}_c})]^\phi \exp\left[\frac{k_1^2}{4k_2} (1-\phi)\right], \end{aligned} \quad (21)$$

where

$$\phi = \frac{1}{1 + 2k_2(\beta_{\theta_d}^2 + \beta_{\theta_c}^2)/b^2}, \quad s_{\hat{\theta}_c} = \left(\frac{\hat{\theta}_c}{a}\right)^{1/b}. \quad (22)$$

### 3.3. Epistemic uncertainty and confidence-based formats

In order to estimate the influence of epistemic uncertainties on the MAF, we need to consider their effect on demand, capacity and hazard and then propagate it to the final  $\lambda_{LS}$  result. First, let the hazard value given the level of IM be a lognormal random variable that varies due to epistemic uncertainty around its median, as represented by multiplying the median  $\hat{H}(s)$  with the random variable  $\varepsilon_{UH}$ :

$$H(s) = \hat{H}(s) \cdot \varepsilon_{UH}, \quad \hat{\varepsilon}_{UH} = 1, \quad \sigma_{\ln \varepsilon_{UH}} = \beta_{UH}. \quad (23)$$

In the above equations and all the discussions to follow, a bar denotes the mean, a hat the median,  $\sigma_x$  is the standard deviation of  $x$  and subscript  $U$  symbolizes epistemic uncertainty.

Inserting the above definition in the expressions we have found for  $\lambda_{LS}$  should make it possible to derive its probabilistic distribution under seismic hazard uncertainty. It is easy to realize that introducing the lognormal  $H(s)$  makes  $\lambda_{LS}$  become lognormally distributed as well. The mean MAF estimate is found by replacing all variants of  $H(s)^p$ ,  $H(s)^\phi$  in pertinent equations with their mean value. The mean of a lognormal variable raised to a power can be estimated [15, Appx A] as:

$$\begin{aligned} \overline{[H(s)]^p} &= [\hat{H}(s)]^p \cdot \exp(0.5p^2\beta_{UH}^2) \\ &= [\hat{H}(s) \cdot \exp(0.5p\beta_{UH}^2)]^p \\ &\approx [\overline{H}(s)]^p \end{aligned} \quad (24)$$



The above approximation by the mean hazard curve is accurate only when  $p, \phi \approx 1$ , i.e., when  $k_2$  is relatively close to zero and thus the curvature of the hazard function is low. This is the case for most ranges of application. Otherwise, as  $p, \phi < 1$  the approximation becomes conservative. At low values of  $p$  or  $\phi$ , for example less than 0.85, it is advisable to employ the first or second form of Equation (24) for improved accuracy. Our hesitation to do so directly stems from the fact that, compared to the mean hazard, its median and dispersion may not always be readily available.

Estimating the mean MAF due to structural uncertainty can be a complex affair if it is deemed capable of influencing the central value of demand and capacity distributions. Instead, we will adopt the typical first-order assumption [3] discussed earlier, stipulating that only the dispersion of structural demand and capacity are influenced. Consequently, let  $s_c, \theta, \theta_c$  be lognormal random variables that vary around their respective medians due to both aleatory and epistemic sources:

$$\begin{aligned} s_c &= \hat{s}_c \cdot \varepsilon_{USc} \cdot \varepsilon_{Sc}, & \hat{\varepsilon}_{USc} &= 1, & \sigma_{\ln \varepsilon_{USc}} &= \beta_{USc}, & \sigma_{\ln \varepsilon_{Sc}} &= \beta_{Sc} \\ \theta &= \hat{\theta} \cdot \varepsilon_{U\theta d} \cdot \varepsilon_{\theta d}, & \hat{\varepsilon}_{U\theta d} &= 1, & \sigma_{\ln \varepsilon_{U\theta d}} &= \beta_{U\theta d}, & \sigma_{\ln \varepsilon_{\theta d}} &= \beta_{\theta d} \\ \theta_c &= \hat{\theta}_c \cdot \varepsilon_{U\theta c} \cdot \varepsilon_{\theta c}, & \hat{\varepsilon}_{U\theta c} &= 1, & \sigma_{\ln \varepsilon_{U\theta c}} &= \beta_{U\theta c}, & \sigma_{\ln \varepsilon_{\theta c}} &= \beta_{\theta c} \end{aligned} \quad (25)$$

As already mentioned, the expressions that have been derived for  $\lambda_{LS}$  so far can directly incorporate epistemic uncertainty by appropriately modifying the corresponding dispersions. To do so explicitly, we shall replace  $p$  and  $\phi$  in all expressions by their respective counterparts  $p'$  and  $\phi'$ :

$$p' = \frac{1}{1 + 2k_2 (\beta_{Sc}^2 + \beta_{USc}^2)} \quad (26)$$

$$\phi' = \frac{1}{1 + 2k_2 (\beta_{\theta d}^2 + \beta_{\theta c}^2 + \beta_{U\theta d}^2 + \beta_{U\theta c}^2) / b^2}. \quad (27)$$

Thus, in order to estimate  $\bar{\lambda}_{LS}$ , the overall mean estimate of  $\lambda_{LS}$  with regard to epistemic uncertainty, we only need to introduce the approximation of Equation (24) and  $p', \phi'$  in Equations (13) and (21) to obtain:

$$\bar{\lambda}_{LS} = \sqrt{p'} k_0^{1-p'} [\bar{H}(\hat{s}_c)]^{p'} \exp \left[ \frac{k_1^2}{4k_2} (1-p') \right] \quad (28)$$

$$\bar{\lambda}_{LS} = \sqrt{\phi'} k_0^{1-\phi'} [\bar{H}(s_{\hat{\theta}_c})]^{\phi'} \exp \left[ \frac{k_1^2}{4k_2} (1-\phi') \right]. \quad (29)$$

The above equations can be thought of being estimates of  $\lambda_{LS}$  at a confidence level consistent with the mean, i.e., somewhat above 50%. For producing estimates of  $\lambda_{LS}$  at user-defined confidence levels, we will follow the SAC/FEMA paradigm: Seismic hazard uncertainty is incorporated directly in  $\lambda_{LS}$  and does not participate in the estimation of confidence-level values. The application of confidence is restricted to structural engineering quantities, making it a vehicle for characterizing model uncertainty (e.g., as related to type, parameters, mechanisms, capacities etc). Thus, the mean MAF estimate due to seismic hazard uncertainty will be introduced directly via Equation (24) and we will seek to estimate the entire distribution of  $\lambda_{LS}$  due to  $\varepsilon_{USc}$  or  $\varepsilon_{U\theta d}$  and  $\varepsilon_{U\theta c}$  of Equation (25) for the IM and EDP basis, respectively. The effect of the aleatory parts has already been taken into account in deriving  $\lambda_{LS}$ . Hence, for the IM-basis, Equation (13) becomes:

$$\begin{aligned} \lambda_{LS} &= \sqrt{p} k_0^{1-p} \left\{ k_0 \exp \left[ -k_2 \ln^2(\hat{s}_c \varepsilon_{USc}) - k_1 \ln(\hat{s}_c \varepsilon_{USc}) \right] \right\}^p \exp \left[ \frac{k_1^2}{4k_2} (1-p) \right] \\ &= \sqrt{p} k_0^{1-p} [\bar{H}(\hat{s}_c)]^p \exp \left[ \frac{k_1^2}{4k_2} (1-p) \right] \cdot \underbrace{\varepsilon_{USc}^{-p(k_1+2k_2 \ln \hat{s}_c)}}_{\text{term A}} \cdot \underbrace{\exp(-pk_2 \ln^2 \varepsilon_{USc})}_{\text{term B}}. \end{aligned} \quad (30)$$

The indicated terms A and B, are the random components that give rise to the variability of  $\lambda_{LS}$  around its central value. Term A is obviously a lognormal variable raised to a power and thus it

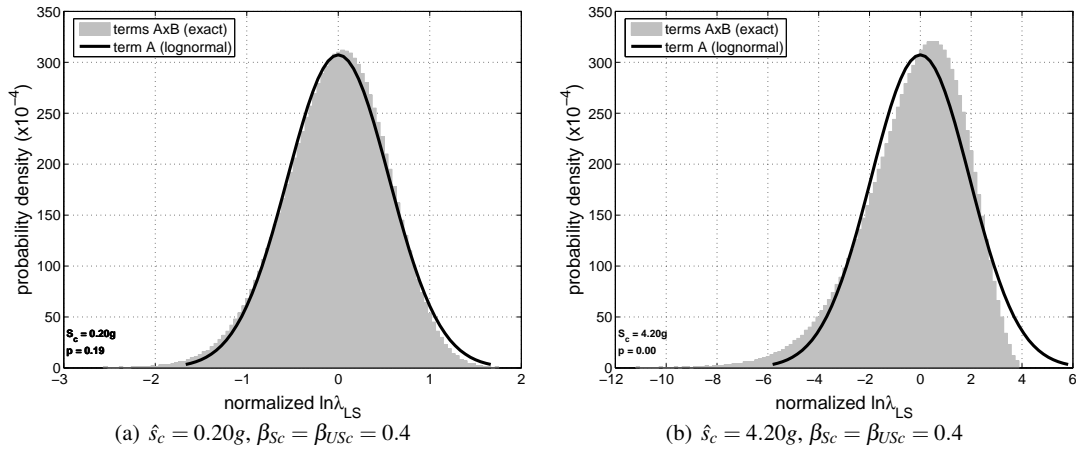


Figure 5. Distributions of  $\lambda_{LS}$  for the hazard curve of Figure 2: (a) At low curvatures it resembles the lognormal term A, while (b) at higher curvatures term B enforces a distinctive skewness. Kolmogorov-Smirnov tests [13] offer confirmation with p-values of 0.19 and nearly zero, respectively.

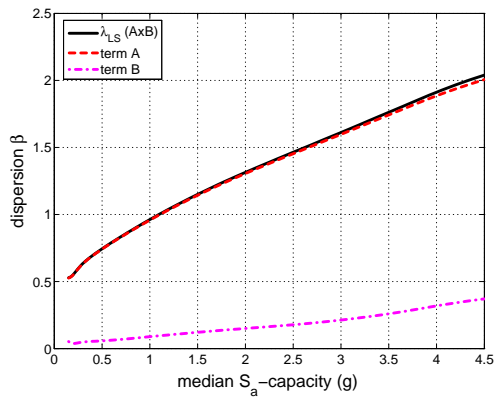


Figure 6. Breakdown of  $\lambda_{LS}$  dispersion.

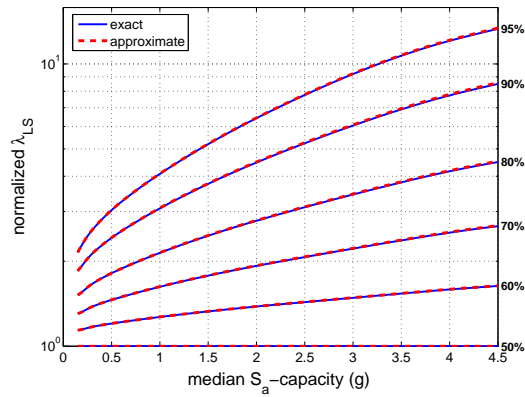


Figure 7. Exact and approximate  $\lambda_{LS}^x$  percentiles.

is also lognormal [15]. Term B involves the exponential of the square of a normal variable and cannot be tackled analytically; Monte Carlo simulation has been employed instead to ascertain its influence. Apparently, it depends on the curvature of the hazard function, as represented by  $k_2$ : When  $k_2$  is relatively low, term B dominates and the  $\lambda_{LS}$  distribution is practically lognormal (Figure 5(a)). If  $k_2$  is high, as occurs for large  $\hat{\delta}_c$  values, then term B imparts a distinctive skewness by stretching the left tail of the distribution (Figure 5(b)). Still, term B does not influence neither the median nor the dispersion of  $\lambda_{LS}$ , as Figure 6 proves. Thus, the dispersion of  $\lambda_{LS}$  is approximated as:

$$\beta_{TUSc} = \beta_{USc} p (k_1 + 2k_2 \ln \hat{\delta}_c). \quad (31)$$

Note that  $\beta_{TUSc}$  is the product of  $p$ , the local hazard slope ( $k_1 + 2k_2 \ln \hat{\delta}_c$ ) and  $\beta_{USc}$ . Thus, it retains the general composition of the SAC/FEMA original and reverts to it when  $k_2 = 0$ .

The median of the distribution (formally the median estimate of the mean  $\lambda_{LS}$ ) is readily available from previous expressions for  $\lambda_{LS}$  if the relevant  $\beta$  dispersions are taken to indicate only aleatory randomness. Having the median and the dispersion should be enough to estimate any  $x$ -percentile value  $\lambda_{LS}^x$ , were it not for the skewness introduced by term A. This effectively makes any high-confidence estimate become exceedingly large for  $x > 0.75$ . Using extensive Monte Carlo simulations, a precise skewness correction factor  $\gamma_x$  is introduced:

$$\gamma_{Sx} = k_2 \beta_{USc}^2 p \cdot \frac{(1-2x)^2}{(1-x)^{0.4}}. \quad (32)$$

The estimate of  $\lambda_{LS}$  at an  $x\%$  confidence level (i.e., the value with an  $x\%$  probability of not being exceeded) now becomes:

$$\lambda_{LS}^x = \sqrt{p} k_0^{1-p} [\overline{H}(\hat{s}_c)]^p \cdot \exp \left[ \frac{k_1^2}{4k_2} (1-p) + K_x \beta_{TUSc} - \gamma_{Sx} \right]. \quad (33)$$

$K_x$  is the standard normal variate corresponding to the desired confidence level. Formally,  $K_x = \Phi^{-1}(x)$ , where  $\Phi^{-1}(\cdot)$  is the inverse CDF of a standard normal variable [13], readily available in any probability textbook or spreadsheet program. For example,  $K_x = 1.28$  for a 90%-confidence estimate. As Figure 7 testifies, the skewness-corrected lognormal distribution that has been adopted offers remarkable accuracy for any value of dispersion,  $k_1$  or  $k_2$  and any percentile, at least up to  $x = 0.95$ .

For the EDP-basis, the same steps shall be followed:

$$\lambda_{LS} = \sqrt{\phi} k_0^{1-\phi} [\overline{H}(s_{\hat{\theta}_c})]^\phi \exp \left[ \frac{k_1^2}{4k_2} (1-\phi) \right] \cdot (\varepsilon_{U\theta c} \varepsilon_{U\theta d})^{-\frac{\phi}{b}(k_1+2k_2 \ln s_{\hat{\theta}_c})} \cdot \exp \left[ -\frac{\phi}{b} k_2 \ln^2 (\varepsilon_{U\theta c} \varepsilon_{U\theta d}) \right]. \quad (34)$$

In analogy to the IM-case, the  $\lambda_{LS}$  dispersion and skewness-correction factor are

$$\beta_{TU\theta} = \beta_{U\theta} \frac{\phi}{b} (k_1 + 2k_2 \ln s_{\hat{\theta}_c}), \quad (35)$$

$$\gamma_{\theta x} = k_2 \beta_{U\theta}^2 \frac{\phi}{b} \cdot \frac{(1-2x)^2}{(1-x)^{0.4}}, \quad (36)$$

where  $\beta_{U\theta}^2 = \beta_{U\theta d}^2 + \beta_{U\theta c}^2$  if no correlation exists between the uncertain demand and capacity. Finally:

$$\lambda_{LS}^x = \sqrt{\phi} k_0^{1-\phi} [\overline{H}(s_{\hat{\theta}_c})]^\phi \exp \left[ \frac{k_1^2}{4k_2} (1-\phi) + K_x \beta_{TU\theta} - \gamma_{\theta x} \right]. \quad (37)$$

Note that in both Equations (33) and (37) epistemic uncertainty appears only via the  $\beta_{TUSc}$  and  $\beta_{TU\theta}$  dispersions. Therefore, the  $p, \phi$  terms are used for deriving percentile  $\lambda_{LS}^x$  values. This is in contrast to the mean-value estimates of Equations (28) and (29) that employ  $p', \phi'$  instead.

### 3.4. Inverting the MAF format

It may be desirable to estimate the value of capacity that will generate a given MAF. To do so, the MAF formats derived earlier need to be inverted. Due to the common form of Equations (13), (21), (33) and (37), the inversion can be performed jointly: We will use (13) as our guide to derive similar results for the other expressions. First it will be transformed to a quadratic equation:

$$(pk_2) \ln^2 \hat{s}_c + (pk_1) \ln \hat{s}_c + \left[ \ln \frac{\lambda_{LS}}{k_0 \sqrt{p}} - \frac{k_1^2}{4k_2} (1-p) \right] = 0 \quad (38)$$

The discriminant is

$$\Delta = p \left( k_1^2 - 4k_2 \ln \frac{\lambda_{LS}}{k_0 \sqrt{p}} \right) \quad (39)$$

which is always positive as  $0 < p \leq 1$ ,  $k_1, k_2, k_3 > 0$  and  $\lambda_{LS} < 1$  for any limit-state of engineering significance. This allows for two solutions for  $\ln \hat{s}_c$ , namely  $R_1 \leq R_2$ , of which the lower one is always negative. Since by nature of the approximation we want a solution on the rightmost descending branch of the fitted parabola in log-log space (Figure 2), we are only interested in the

higher of the two. Thus:

$$\hat{s}_c = \exp \left[ \frac{1}{2k_2} \left( -k_1 + \sqrt{\frac{k_1^2}{p} - \frac{4k_2}{p} \ln \frac{\lambda_{LS}}{k_0 \sqrt{p}}} \right) \right] \quad (40)$$

If we are interested in the corresponding  $\hat{\theta}_c$  then:

$$\hat{\theta}_c = a \cdot \exp \left[ \frac{b}{2k_2} \left( -k_1 + \sqrt{\frac{k_1^2}{\phi} - \frac{4k_2}{\phi} \ln \frac{\lambda_{LS}}{k_0 \sqrt{\phi}}} \right) \right]. \quad (41)$$

To introduce a confidence basis for estimation, we need to start from Equations (33) and (37). The derivation mildly differs from above due to the  $\beta_{TUSc}$ ,  $\beta_{TU\theta}$  terms that contain  $\hat{s}_c$  and  $\hat{\theta}_c$ , the variables we want to solve for. After expanding them and collecting terms the same steps can be employed to arrive at the following results:

$$\hat{s}_c = \exp \left[ K_x \beta_{USc} + \frac{1}{2k_2} \left( -k_1 + \sqrt{\frac{k_1^2}{p} - \frac{4k_2}{p} \left( \ln \frac{\lambda_{LS}^x}{k_0 \sqrt{p}} + \gamma_{Sx} \right) + 4k_2^2 K_x^2 \beta_{USc}^2} \right) \right], \quad (42)$$

$$\hat{\theta}_c = a \cdot \exp \left[ K_x \beta_{U\theta} + \frac{b}{2k_2} \left( -k_1 + \sqrt{\frac{k_1^2}{\phi} - \frac{4k_2}{\phi} \left( \ln \frac{\lambda_{LS}^x}{k_0 \sqrt{\phi}} + \gamma_{\theta x} \right) + \frac{4k_2^2}{b^2} K_x^2 \beta_{U\theta}^2} \right) \right]. \quad (43)$$

#### 4. DEMAND-CAPACITY FACTORED DESIGN FORMAT

The Demand-Capacity Factor Design (DCFD) format allows simple safety checks for any limit-state. Let's say that we wish to verify whether the structure complies with a limit-state performance objective  $P_o$ , for example the typical 10% in 50yrs for Life Safety corresponding to an allowable MAF of  $P_o = -\ln(1 - 0.10)/50 = 0.00211$  or a minimum mean return period of  $1/P_o \approx 475$ yrs. In such an assessment, we need to estimate the median demand  $\hat{\theta}_{po}$  and associated dispersion  $\beta_{\theta d}$  that are representative of  $P_o$ . This entails statistically summarizing the EDP results from several nonlinear dynamic analyses using ground motion records having (or scaled to) an intensity level  $s_{po} = H^{-1}(P_o)$ , where  $H^{-1}(\cdot)$  is the inverse of the hazard function. Essentially, this amounts to estimating the distribution of EDP values from the appropriate horizontal "stripe" [15] cutting through the IDA curves of, e.g., Figure 1. Given the typical assumptions about the lognormality of the EDP capacity and the conditional EDP demand, Cornell *et al.* [3] proved that safety can be verified as

$$\hat{\theta}_c \exp \left( -\frac{k_1}{2b} \beta_{\theta c}^2 \right) \geq \hat{\theta}_{po} \exp \left( \frac{k_1}{2b} \beta_{\theta d}^2 \right). \quad (44)$$

An exponential factor can be appended at the right side of Equation (44) to offer a choice of treating the effect of epistemic uncertainties at the desired  $x$ -confidence level:

$$\hat{\theta}_c \exp \left( -\frac{k_1}{2b} \beta_{\theta c}^2 \right) \geq \hat{\theta}_{po} \exp \left( \frac{k_1}{2b} \beta_{\theta d}^2 + K_x \beta_{U\theta} \right), \quad (45)$$

where  $\beta_{U\theta}^2 = \beta_{U\theta d}^2 + \beta_{U\theta c}^2$  is the total uncertainty in demand and capacity. Let us now investigate how the DCFD format changes when the second-order approximation of Equation (9) is introduced.

#### 4.1. Mean-value-based DCFD format

Safety checking is basically performed by comparing the limit-state MAF with the maximum allowable value  $P_o$ :

$$\begin{aligned} P_o \geq \lambda_{LS} &\Leftrightarrow \frac{P_o}{k_0 \sqrt{p}} \geq \exp(-pk_2 \ln^2 \hat{s}_c - pk_1 \ln \hat{s}_c) \exp\left[\frac{k_1^2}{4k_2}(1-p)\right] \\ &\Leftrightarrow (pk_2) \ln^2 \hat{s}_c + (pk_1) \ln \hat{s}_c + \left(\ln \frac{P_o}{k_0 \sqrt{p}} - \frac{k_1^2}{4k_2}(1-p)\right) \geq 0 \\ &\Leftrightarrow pk_2(\ln \hat{s}_c - R_1)(\ln \hat{s}_c - R_2) \geq 0, \end{aligned} \quad (46)$$

where  $R_1, R_2$  ( $R_1 \leq R_2$ ) are the two solutions of the quadratic equation that were derived in the previous section. Since we are only interested in solutions appearing in the rightmost descending branch of the parabolic fit (Figure 2),  $\ln \hat{s}_c$  will always be larger than  $R_1$ . Therefore, the first two terms in Equation (46) are positive and the solution is governed by the third. The inequality becomes:

$$\ln \hat{s}_c \geq \frac{1}{2k_2} \left( -k_1 + \sqrt{\frac{k_1^2}{p} - \frac{4k_2}{p} \ln \frac{P_o}{k_0 \sqrt{p}}} \right). \quad (47)$$

The above equation can form the basis for a checking format, although it lacks the elegance and simplicity of the original SAC/FEMA expression. Further simplifications are in order. If we replace the target performance objective  $P_o$  with its corresponding level of IM =  $s_{po}$  via the hazard fit, then

$$\begin{aligned} \ln \hat{s}_c &\geq \frac{1}{2k_2} \left[ -k_1 + \sqrt{\frac{k_1^2}{p} + \frac{4k_2}{p} (k_1 \ln s_{po} + k_2 \ln^2 s_{po} + \ln \sqrt{p})} \right] \\ &\Leftrightarrow k_1 + 2k_2 \ln \hat{s}_c \geq p^{-0.5} \sqrt{(k_1 + 2k_2 \ln s_{po})^2 + 2k_2 \ln p}. \end{aligned} \quad (48)$$

Since  $0 < p \leq 1$  and  $k_2 \geq 0$ , the last term,  $2k_2 \ln p$ , in the square root is negative or zero. Therefore, a stronger (more conservative) statement than the above will be generated if this term is removed. Further, the expression inside the square is positive:  $(k_1 + 2k_2 \ln s)$  is actually the negative of the first derivative of the hazard approximation. As the parabolic fit always presents negative slopes on its valid right side (Figure 2), the nested square cancels out the root:

$$\begin{aligned} k_1 + 2k_2 \ln \hat{s}_c &\geq p^{-0.5} (k_1 + 2k_2 \ln s_{po}) \Leftrightarrow \\ \hat{s}_c &\geq (s_{po})^{1/\sqrt{p}} \exp\left[\frac{k_1}{2k_2} \left(\frac{1}{\sqrt{p}} - 1\right)\right]. \end{aligned} \quad (49)$$

Note that  $\exp(\cdot)$  is a monotonically increasing function, therefore the inequality is preserved when deriving the above final result.

For an EDP-based format,  $p$  and  $\hat{s}_c$  are replaced by  $\phi$  and  $s_{\hat{\theta}_c}$ , respectively. Employing the power-law approximation of Equation (14) to express the IM-values  $s_{\hat{\theta}_c}$  and  $s_{po}$  as functions of  $\hat{\theta}_c$  and  $\hat{\theta}_{po}$  produces:

$$\hat{\theta}_c \geq (\hat{\theta}_{po})^{1/\sqrt{\phi}} \exp\left[\left(\frac{bk_1}{2k_2} - \ln a\right) \left(\frac{1}{\sqrt{\phi}} - 1\right)\right]. \quad (50)$$

#### 4.2. Confidence-based DCFD format

In order to introduce a confidence-basis for estimation, we need to repeat the process shown in the previous section, starting with Equation (46) and using the solutions provided by Equations (42), (43). Then we arrive at the equivalent of Equation (48) with confidence terms included:

$$k_1 + 2k_2 \ln \hat{s}_c \geq 2k_2 K_x \beta_{USc} + \frac{1}{\sqrt{p}} \sqrt{(k_1 + 2k_2 \ln s_{po})^2 + 2k_2 \ln p - 4k_2 \gamma_{Sx} + p (2k_2 K_x \beta_{USc})^2} \quad (51)$$

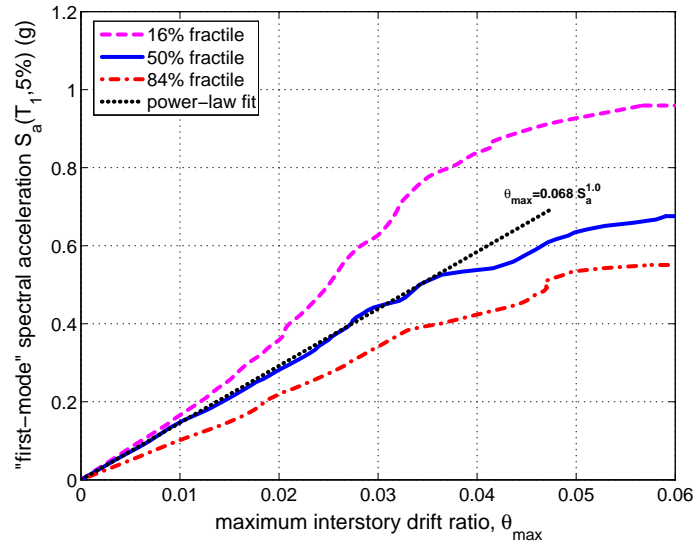


Figure 8. 16, 50, 84% fractile IDA curves and the median EDP given IM power-law fit for the 9-story steel moment-resisting frame.

Luckily, the last three terms under the square root have very low values compared to the first (square) term and nearly cancel out each other: Extensive tests have shown that the value of the square root only changes by 1–2% when they are excluded, for the practical range of all the parameters included. Therefore, Equation (51) can be simplified:

$$k_1 + 2k_2 \ln \hat{s}_c \geq 2k_2 K_x \beta_{USc} + \frac{1}{\sqrt{p}} (k_1 + 2k_2 \ln s_{po}) \Leftrightarrow$$

$$\hat{s}_c \geq (s_{po})^{1/\sqrt{p}} \exp \left[ \frac{k_1}{2k_2} \left( \frac{1}{\sqrt{p}} - 1 \right) + K_x \beta_{USc} \right]. \quad (52)$$

Similarly, for the EDP basis:

$$\hat{\theta}_c \geq (\hat{\theta}_{po})^{1/\sqrt{\phi}} \exp \left[ \left( \frac{bk_1}{2k_2} - \ln a \right) \left( \frac{1}{\sqrt{\phi}} - 1 \right) + K_x \beta_{U\theta} \right]. \quad (53)$$

Strictly speaking, it may be argued that Equations (52), (53) do not deserve the DCFD name, without having separate demand and capacity factors. Still, this is only a technicality since they serve the exact same purpose as the SAC/FEMA original Equation (45) and they do so with significantly improved accuracy. Therefore, we can claim them to be worthy successors.

## 5. APPLICATION EXAMPLES

A number of simple calculations will be demonstrated using the closed-form solutions. Our testbed is the LA9 nine-story steel moment-resisting frame ( $T_1 = 2.35s$ ), as modelled by Vamvatsikos and Fragiadakis [8]. Pertinent analysis results in the form of IDA curves and capacity points appear in Figure 1 and are also summarized in Figure 8. The estimated IM and EDP capacities are expressed in terms of the first-mode spectral acceleration  $S_a(T_1, 5\%)$  and the maximum interstory drift ratio  $\theta_{max}$ , respectively. Their distributions are both lognormal, as confirmed by a Kolmogorov-Smirnov test [13]. The corresponding parameters are  $\hat{s}_c = 0.42g$ ,  $\beta_{Sc} = 43\%$ ,  $\beta_{USc} = 25\%$  and  $\hat{\theta}_c = 0.03$ ,  $\beta_{\theta c} = 30\%$ ,  $\beta_{U\theta c} = 25\%$ . The mean hazard curve estimated for Van Nuys, CA for  $S_a(2.35s, 5\%)$  will be employed for all subsequent calculations. In all cases, fitting of the hazard approximations will be performed as in Figure 2, i.e., tangentially for the first-order solution and capturing mainly

lower MAF values for the second-order fit [9]. To showcase the wide-IM validity of the latter, the same fit will be employed throughout this section, parameterized by  $k_0 = 4.75 \cdot 10^{-5}$ ,  $k_1 = 4.12$ ,  $k_2 = 0.497$ . Instead, the first-order solution will be refitted each time.

First, let us try a simple MAF assessment for the aforementioned capacity. If an IM-basis solution via Equation (28) is sought, then  $p' = 0.8025$  and the mean  $\lambda_{LS}$  is estimated as:

$$\bar{\lambda}_{LS} = \sqrt{p'} k_0^{1-p'} [\bar{H}(\hat{s}_c)]^{p'} \exp \left[ \frac{k_1^2}{4k_2} (1-p') \right] = 0.00298.$$

The result of numerical integration comes to 0.00295, indicating an error of only 1%. On the other hand, a first-order result via Equation (8) and for  $k_1 = 3.48$  provides  $\bar{\lambda}_{LS} = 0.0050$ , a 70% overestimation.

Use of the EDP-based formats requires the limit-state of interest to reside away from global collapse due to the approximation of Equation (14). A practical rule of thumb is requiring no more than 16% collapses to occur in nonlinear dynamic analyses that have been performed under different ground motions at the range of intensities corresponding to the limit-state, i.e., close to the level of  $\hat{s}_c$ . The 84% fractile curve in Figure 8 indicates that this is valid for intensities up to 0.55g or median EDP capacities of up to 0.043. This being higher than  $\hat{\theta}_c = 0.03$ , an EDP-basis result can be accurately estimated by Equation (29). The needed parameters are  $\phi' = 0.781$  and  $s_{\hat{\theta}_c} = 0.438$  to provide a value of

$$\bar{\lambda}_{LS} = \sqrt{\phi'} k_0^{1-\phi'} [\bar{H}(s_{\hat{\theta}_c})]^{\phi'} \exp \left[ \frac{k_1^2}{4k_2} (1-\phi') \right] = 0.00296$$

that is practically the same as before. The first-order result from Equation (15) is 0.0053 which again becomes a gross overestimation.

Estimates with an  $x = 90\%$  confidence of not been exceeded can be obtained via Equation (33) for the IM-basis. The intermediate values needed for the calculation come out as  $p = 0.845$ ,  $K_x = 1.28$ ,  $\beta_{TUSc} = 0.687$  and  $\gamma_{Sx} = 0.042$ . Then

$$\lambda_{LS}^{90\%} = \sqrt{p} k_0^{1-p} [\bar{H}(\hat{s}_c)]^p \cdot \exp \left[ \frac{k_1^2}{4k_2} (1-p) + K_x \beta_{TUSc} - \gamma_{Sx} \right] = 0.0056,$$

a result obviously higher than the mean that again is practically indistinguishable from the numerical answer.

Let us now view this problem from a different perspective, closer to a design rather than an assessment situation. We do not possess a nonlinear model of the structure, therefore the results of Figure 8 are not available. Still, for a long-period structure, the equal displacement rule dictates that  $b = 1$ , while the coefficient  $a = 0.068$  may be estimated by elastic response spectrum analysis using a few ground motion records or, perhaps, the code design spectrum. It may be of interest to find for such a structure what drift capacity is required to satisfy a Life Safety performance objective of 10% in 50yrs, i.e., not exceeding a MAF of  $P_o = 0.00211$ . Obviously, our previous results show that  $\hat{\theta}_c = 0.03$  is not enough. Assuming the same dispersions apply, we can use Equation (43) with  $\beta_{\theta d} = 0.3$ ,  $\beta_{U\theta d} = 0.2$ ,  $\beta_{U\theta} = 0.32$ ,  $\phi = 0.848$ ,  $\gamma_{\theta x} = 0.0695$ , to calculate an estimate consistent with a 90% confidence:

$$\hat{\theta}_c = a \cdot \exp \left[ K_x \beta_{U\theta} + \frac{b}{2k_2} \left( -k_1 + \sqrt{\frac{k_1^2}{\phi} - \frac{4k_2}{\phi} \left( \ln \frac{P_o}{k_0 \sqrt{\phi}} + \gamma_{\theta x} \right) + \frac{4k_2^2}{b^2} K_x^2 \beta_{U\theta}^2} \right) \right] \\ = 0.045.$$

Similarly, for  $\gamma_{\theta x} = K_x = 0$  we get a 50% estimate of 0.030 that happens to be the same as the  $\hat{\theta}_c$  we originally assumed.

Let's say that the structure goes through a design cycle and, e.g., via static pushover analysis, we confirm that a capacity of 0.040 has been provided instead; more than the 50% estimate but



obviously less than the 0.045 required at a 90% level. Would that be adequate at the 10% in 50yrs level if we only require a confidence of 75%? Such a simple check can be performed in a design situation without knowledge of the full IDA results of Figure 8. We can simply subject the structural model to a few dynamic analyses using ground motions consistent with an intensity of  $S_d(T_1, 5\%) = H^{-1}(P_o) = 0.347g$ . The corresponding median response is thus estimated to be  $\hat{\theta}_{po} = 0.024$  with a dispersion of  $\beta_{\theta d} = 0.31$ . Then, with  $K_x = 0.675$ , Equation (53) becomes:

$$\hat{\theta}_c \geq (\hat{\theta}_{po})^{1/\sqrt{\phi}} \exp \left[ \left( \frac{bk_1}{2k_2} - \ln a \right) \left( \frac{1}{\sqrt{\phi}} - 1 \right) + K_x \beta_{U\theta} \right] \Leftrightarrow$$

$$0.040 \geq 0.0384$$

thus positively answering our question. Had we used the more accurate Equation (43) the factored demand (i.e., the right side of the inequality) would become 0.0374 instead, practically matching the numerical result and indicating a slightly conservative error of less than 3%. Still, the DCFD inequality above is a vastly more flexible format, as it factually links the demand  $\hat{\theta}_{po}$  with the capacity  $\hat{\theta}_c$  and it can be solved for either of the two. Combined with the wide-range validity of the second-order hazard fit, it can help us provide answers to fundamental design issues.

## 6. CONCLUSIONS

Novel SAC/FEMA closed-form solutions have been presented that take advantage of a second-order power-law hazard fit to outperform their predecessors for the evaluation of seismic performance. The expressions derived are fully compatible with the original ones, allowing both the estimation of the mean annual frequency of limit-state exceedance and the LRFD-style checking of limit-state safety. Both an engineering demand parameter basis and an intensity measure basis are possible, covering all possible fields of use. Most importantly, by including the overwhelming effect of the hazard function curvature, the new expressions practically eliminate the most significant errors in the original format, achieving robustness regardless of the hazard curve shape. Other, lesser sources of error may still remain, yet the improvement offered cannot be understated. Both design and assessment calculations can now be undertaken without the need for numerical integration, even allowing (previously impractical) inverse estimates of allowable demand or required capacity. Such capabilities will, hopefully, pave the way for incorporation into new practically-minded frameworks and, eventually, seismic guidelines.

## ACKNOWLEDGEMENT

The author gratefully acknowledges the support of the European Research Executive Agency via Marie Curie grant PCIG09-GA-2011-293855.

## REFERENCES

1. SAC/FEMA. Recommended seismic design criteria for new steel moment-frame buildings. *Report No. FEMA-350*, SAC Joint Venture, Federal Emergency Management Agency, Washington, DC, 2000.
2. SAC/FEMA. Recommended seismic evaluation and upgrade criteria for existing welded steel moment-frame buildings. *Report No. FEMA-351*, prepared for the Federal Emergency Management Agency, Washington, DC, 2000.
3. Cornell CA, Jalayer F, Hamburger RO, Foutch DA. The probabilistic basis for the 2000 SAC/FEMA steel moment frame guidelines. *ASCE Journal of Structural Engineering* 2002; **128**(4):526–533.
4. AISC. *LRFD Manual of Steel Construction, 3rd edition*. American Institute of Steel Construction: Chicago, IL, 2003.
5. Fajfar P, Dolsek M. A practice-oriented estimation of the failure probability of building structures. *Earthquake Engineering and Structural Dynamics* 2012; **41**(3):531–547.
6. Franchin P, Pinto P. Method for probabilistic displacement-based design of RC structures. *ASCE Journal of Structural Engineering* 2012; **138**(5):585–591.
7. Cornell CA, Krawinkler H. Progress and challenges in seismic performance assessment. *PEER Center News* 2000; **3**(2). URL <http://peer.berkeley.edu/news/2000spring/index.html>. [May 2012].

8. Vamvatsikos D, Fragiadakis M. Incremental dynamic analysis for estimating seismic performance sensitivity and uncertainty. *Earthquake Engineering and Structural Dynamics* 2010; **39**(2):141–163.
9. Dolsek M, Fajfar P. The effect of masonry infills on the seismic response of a four storey reinforced concrete frame—a probabilistic assessment. *Engineering Structures* 2008; **30**(11):3186–3192.
10. Vamvatsikos D, Cornell CA. Incremental dynamic analysis. *Earthquake Engineering and Structural Dynamics* 2002; **31**(3):491–514.
11. Aslani H, Miranda E. Probability-based seismic response analysis. *Engineering Structures* 2005; **27**(8):1151–1163.
12. Bradley BA, Dhakal RP. Error estimation of closed-form solution for annual rate of structural collapse. *Earthquake Engineering and Structural Dynamics* 2008; **37**(15):1721–1737.
13. Benjamin JR, Cornell CA. *Probability, Statistics, and Decision for Civil Engineers*. McGraw-Hill: New York, 1970.
14. Vamvatsikos D, Dolsek M. Equivalent constant rates for performance-based assessment of ageing structures. *Structural Safety* 2011; **33**(1):8–18.
15. Jalayer F. Direct probabilistic seismic analysis: Implementing non-linear dynamic assessments. PhD Dissertation, Department of Civil and Environmental Engineering, Stanford University, Stanford, CA, 2003.
16. Liel AB, Haselton CB, Deierlein GG, Baker JW. Incorporating modeling uncertainties in the assessment of seismic collapse risk of buildings. *Structural Safety* 2009; **31**(2):197–211.
17. Kennedy RC, Short SA. Basis for seismic provisions of DOE-STD-1020. *Report UCRL-CR-111478, S/C - B235302*, Lawrence Livermore National Laboratory, Livermore, CA, 1994.